



HAL
open science

Disclosing the Preferential Mercury Chelation by SeCys Containing Peptides over Their Cys Analogues

Mikel Bernabeu de Maria, Diego Tesauro, Filippo Prencipe, Michele Saviano, Luigi Messori, Christine Enjalbal, Ryszard Lobinski, Luisa Ronga

► **To cite this version:**

Mikel Bernabeu de Maria, Diego Tesauro, Filippo Prencipe, Michele Saviano, Luigi Messori, et al.. Disclosing the Preferential Mercury Chelation by SeCys Containing Peptides over Their Cys Analogues. *Inorganic Chemistry*, 2023, 62 (37), pp.14980-14990. 10.1021/acs.inorgchem.3c01708 . hal-04224425

HAL Id: hal-04224425

<https://univ-pau.hal.science/hal-04224425>

Submitted on 30 Jan 2024

HAL is a multi-disciplinary open access archive for the deposit and dissemination of scientific research documents, whether they are published or not. The documents may come from teaching and research institutions in France or abroad, or from public or private research centers.

L'archive ouverte pluridisciplinaire **HAL**, est destinée au dépôt et à la diffusion de documents scientifiques de niveau recherche, publiés ou non, émanant des établissements d'enseignement et de recherche français ou étrangers, des laboratoires publics ou privés.

Disclosing the preferential mercury chelation by SeCys containing peptides over their Cys analogues

*Mikel Bernabeu de Maria, Diego Tesauero, Filippo Prencipe, Michele Saviano, Luigi Messori,
Christine Enjalbal, Ryszard Lobinski, Luisa Ronga **

Dr. Luisa Ronga, Dr. Ryszard Lobinski, Mikel Bernabeu De Maria-Pays de l'Adour, E2S
UPPA, CNRS, IPREM, 64000 Pau, France.

Prof. D. Tesauero, Pr. F. Rossi- Department of Pharmacy and CIRPeB, Università degli Studi di
Napoli Federico II, 49 80131 Naples, Italy.

Dr. Filippo Prencipe, Dr. Michele Saviano- Istituto di Cristallografia (IC), CNR, 70126 Caserta,
Italy.

Prof. Luigi Messori- Department of Chemistry, Università degli Studi di Firenze, 50019 Sesto
Fiorentino, Italy

Prof. Christine Enjalbal- IBMM, Université de Montpellier, CNRS, ENSCM, UMR 5247, 34293
Montpellier Cedex 5, France.

Dr. Ryszard Lobinski- Warsaw University of Technology, 00-664 Warsaw, Poland.

KEYWORDS

Selenocysteine, mercury, electrospray mass spectrometry, selenopeptide, mercury chelation.

ABSTRACT

Methylmercury, mercury (II) and mercury (I) chlorides were found to react with vasopressin, a nonapeptide hormone cyclized by two cysteine residues, and its mono- and diselenium analogues to form several mercury-peptide adducts. The replacement of Cys by SeCys in vasopressin increased the reactivity towards methylmercury, with the predominant formation of -Se/S-Hg-Se-bridged structures and the consequent demethylation of methylmercury. In competitive experiments, CH₃HgCl reacted preferentially with the diselenium analogue rather than with vasopressin. The diselenium peptide also showed the capability to displace the CH₃Hg-moiety bound to S in vasopressin. These results open a promising perspective for the use of selenopeptides for methylmercury chelation and detoxification strategies.

INTRODUCTION

Mercury (Hg), occurring in a number of inorganic (Hg(0), Hg(I) and Hg(II)) and organic (i.e. CH₃Hg⁺) forms,^{1,2} has been placed by the World Health Organization (WHO) on the list of top 10 most hazardous substances for humans, who are exposed mainly through dietary intake.^{3,4} Mercury is classified as a soft element in the Pearson theory.⁵ The affinity of Hg²⁺ and CH₃Hg⁺ for the thiol group (soft base) of low- and high-molecular weight biological ligands has been considered as the main reason for its high toxicity.⁶

Cysteine (Cys, C) -containing proteins and peptides are the primary targets for Hg²⁺ and CH₃Hg⁺.⁷ The coordination of Hg(II) to Cys is well described and results in the preferential formation of a

stable linear Cys-Hg-Cys complex with the stability constant in the range of 10^{15} - 10^{42} .⁸ The formation of other species displaying tri- and tetragonal geometries was also reported.⁹ Moreover, the complexes formed between Hg(II) and linear and cyclic peptide scaffolds comprising typical metal binding motifs, such as CxCxxC and CxCxC, found in metallothioneins and in the MerR metalloregulatory protein, show that the tri-thiolate coordination (HgCys₃) is the most frequent for these peptides at physiological pH.^{10,11} A preference of Hg(II) for a di-thiolate stoichiometry (Cys-Hg-Cys) was evidenced in multi-cysteinyll peptides by mass spectrometry (MS)¹² and in several elements of Hg(II) transport proteins (MerP, MerT, MerA), while tri- or tetra-coordinations were found in rubredoxin or in the MerR metalloregulatory protein dimer.¹³⁻¹⁷

More recently, it was found by X-ray photoelectron spectroscopy (XPS) that albumin, the main Hg(II)-binding protein in blood plasma, bound Hg(II) through a Cys-Hg-Cys coordination motif, while other Hg binding sites existed within the protein.¹⁸

The affinity of Hg(II) for thiol groups can provide some explanation for Hg toxicity pathways. For example, the close structural resemblance of CH₃Hg-L-cysteine complex with L-methionine¹⁹ was reported to be partially responsible for its transport through the blood-brain and the placental barriers.^{20,21} The covalent CH₃Hg⁺-induced modification of thiol-containing biomolecules (the so-called “S-mercuration”) was claimed responsible for the inactivation of several enzymes, such as the carnitine transporter^{22,23} and the sorbitol dehydrogenase.²⁴ The Cys-mediated binding of CH₃Hg⁺ and Hg²⁺ in proteins was also reported to induce apoptosis modulation by interfering with several metabolic pathways.⁶

The formation of complexes between Cys and Hg(I) has been less studied than that between Cys and Hg(II). Heyrovsky *et al.* postulated the formation of a Cys-Hg-Hg-Cys complex and its

subsequent transformation into Cys-Hg-Cys by addition of Cys, accompanied by the Hg oxidation from Hg(I) to Hg(II).²⁵

Selenocysteine (SeCys, U), the 21st proteinogenic amino acid and the selenium (Se) analogue of cysteine, was also proposed as a Hg(II) target.²⁶ Although sulfur and selenium both belong to the chalcogen group (16), the selenol (-SeH) of SeCys is characterized by a softer character and higher nucleophilicity in comparison with the thiol (-SH) of Cys. Hg(II) affinity for -SeH is ca. 10^6 times larger than that for -SH, revealing selenium as the primary target of CH_3Hg^+ .²⁷ Studies of the formation of complexes of Hg(II) compounds with SeCys have been scarce. Carty *et al.* reported on the characterization of the synthesized $\text{CH}_3\text{Hg-SeCys}$.^{28,29} The synthetic $\text{CH}_3\text{Hg-selenoglutathionate}$ was characterized by NMR and X-Ray spectroscopy and the comparison with its S-analogue didn't show a significant change in the structure.³⁰ The formation of $\text{CH}_3\text{Hg-SeCys}$ complexes was found to be thermodynamically more favorable than that of $\text{CH}_3\text{Hg-Cys}$ compounds by quantum chemical calculations³¹ but no experimental evidence was provided.

SeCys is genetically incorporated into selenoproteins (25 in humans), a class of proteins containing at least one SeCys,³² but examples of the formal identification of the Hg(II)-SeCys moiety in peptide biomolecules have been rare and were limited to high energy-resolution X-ray absorption near-edge structure (HR-XANES).³³ Tetraselenolate $\text{Hg}(\text{SeCys})_4$ was identified in an animal tissue³⁴ while Pickering *et al.* provided conclusive evidence for the binding of CH_3Hg^+ to Se in the selenoenzyme thioredoxin reductase 1 (TrxR1).³⁵ To the best of our knowledge, no selenopeptide model nor mimicry interacting with Hg compounds have been investigated. The comparative reactivity of Hg(II) towards Cys and SeCys has not been explored since the first study of Sugaira *et al.* who used NMR to establish the following order of binding affinity to CH_3Hg^+ : $\text{SeH} > \text{SH} \geq \text{Se-Se} > \text{NH}_2 > \text{SS}$.³⁶

The goal of this research was to investigate by liquid chromatography (LC) coupled to electrospray ultra-high resolution mass spectrometry (ESI-MS) the competitive reactivity of a model disulfide peptide (vasopressin), and its mono- and diselenium analogues (Figure 1) towards methylmercury, mercury (II) and mercury (I) chlorides in the quest of potential mercury detoxification agents. Vasopressin (Figure 1A) is a nonapeptide hormone cyclized by two cysteine residues, best known for its antidiuretic and vasopressor actions. Its diselenide analogue ((Se-Se)-AVP, Figure 1B) was previously described,^{37,38} and its selenylsulfide analogue ((S-Se)-AVP, Figure 1C) was synthesized for the purpose of this study. The elucidation of the Se-Hg binding sites was achieved by fragmentation of the reaction products in the gas phase (MSⁿ),³⁹ as proposed elsewhere for the study of the reactivity of AVP and (Se-Se)-AVP peptides with medically relevant gold compounds.⁴⁰

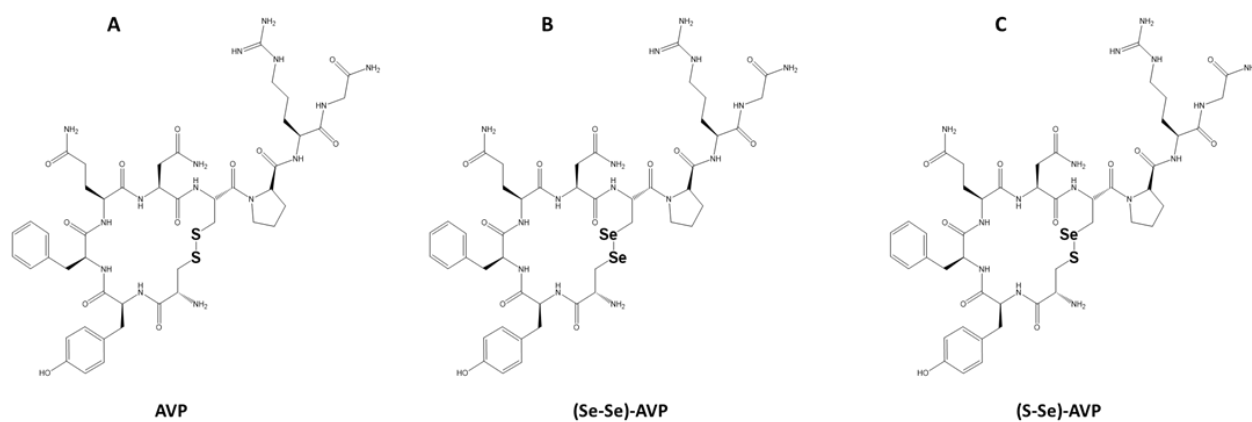


Figure 1. (A) Vasopressin (AVP), (B) its diselenide (Se-Se)-AVP and (C) selenylsulfide (S-Se)-AVP analogues.

EXPERIMENTAL SECTION

Materials

Dithiothreitol (DTT), ammonium acetate, acetic acid, ammoniac, acetonitrile (ACN), methyl mercury chloride (CH_3HgCl) and mercury chloride (HgCl_2) were purchased from Sigma-Aldrich. Formic acid (FA) was purchased from Thermo Fisher Scientific. Mercury(I) chloride (Hg_2Cl_2) was provided by Pr. Luigi Messori.

AVP (98% HPLC purity) was purchased from Eurogenetec . (Se-Se)-AVP (97% HPLC purity) was synthesized as previously described^{37,38} and (S-Se)-AVP (95% HPLC purity) was synthesized as described here.

Fmoc-protected amino acid derivatives, coupling reagents (O-benzotriazole-N,N,N',N'-tetramethyluroniumhexafluorophosphate (HBTU), and Hydroxybenzotriazole (HOBt)), and resin (Rink amide p-methylbenzhydrylamine MBHA 0.78 mmol/g) were purchased from Calbiochem–Novabiochem (Laufelfingen, Switzerland). Seleno-L-cystine, m-Cresol, thioanisole, trifluoroacetic acid, trimethylsilyl, trifluoromethanesulfonate, trifluoroacetic acid, Kaiser test kit, TLC Silica Gel 60 Aluminium sheets and all other solvents and reagents were purchased from Sigma-Aldrich, Steinheim, Germany. For the synthesis of (S-Se)-AVP, all the chemicals were used as received without further purification. As example, the HPLC purity of Fmoc-Gly from Novabiochem was $\geq 99\%$.

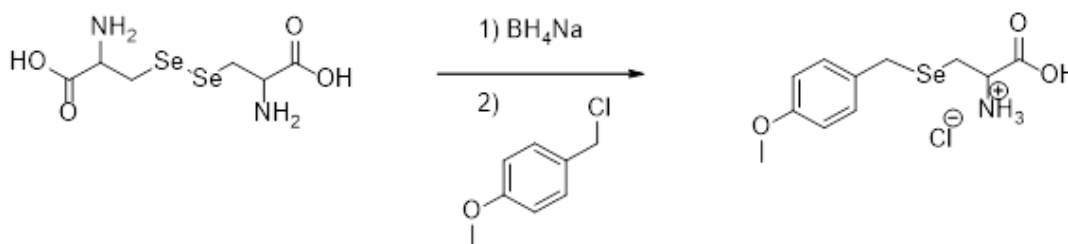
Warning: Methylmercury and other Hg (II) and Hg(I) forms are highly toxic and must be handled with appropriate personal protection. This requires the use of highly-resistant laminate gloves, use of a fume hood, and approved breathing apparatus.

Methods

(S-Se)-AVP peptide synthesis

In order to perform the solid phase synthesis of the (S-Se)-AVP peptide, an orthogonally protected SeCys building block was prepared as reported in Scheme 1 and 2 and then incorporated on the growing peptide chain.

Synthesis of Se-4-methoxybenzylseleno-L-cysteine (SeCys(MBzl))⁴¹

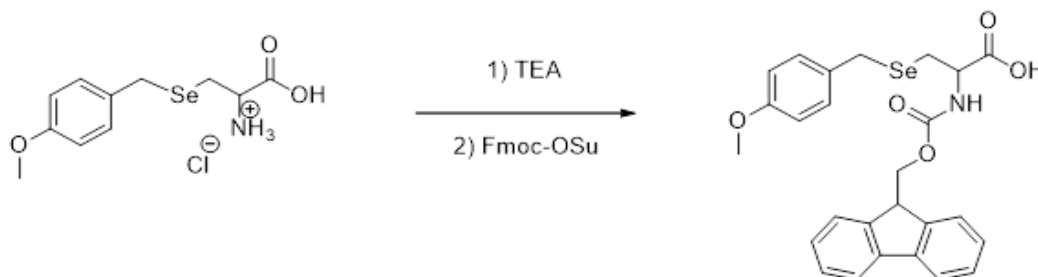


Scheme 1. Synthesis of Se-4-methoxybenzylseleno-L-cysteine from seleno-L-cystine.

Seleno-L-cystine (334 mg, 1 mmol) was suspended in 1 mL of 0.500 M NaOH. The mixture was cooled in an ice bath, then a solution of NaBH_4 (306 mg, 8.1 mmol) dissolved in water (2 mL) was added drop by drop. The reaction is vigorous and develops H_2 (as the reaction proceeds the color changes from yellow to white and gradually a colorless solution was obtained). At the end of the gas evolution, glacial acetic acid was added up to pH 6 (also in this case the reaction is vigorous). *p*-Methoxybenzyl chloride (PMB) (202 μL , 2 mmol) was added drop by drop and the mixture left under stirring at room temperature. The reaction is fast and takes about 30 minutes to complete. It was acidified with HCl 37% to favor the precipitation of the product (cool in an ice bath). The precipitate is filtered and recrystallized from hot water to give a white solid. The pure compound was analyzed by ^1H NMR in $(\text{CD}_3)_2\text{SO}$ (Figure S11) and ESI-MS (Figure S12).

¹H NMR (400 MHz, (CD₃)₂SO DMSO d₆) δ 8.54 (bs, 3H), 7.26 (d, *J* = 8.6 Hz, 2H), 6.87 (d, *J* = 8.7 Hz, 2H), 3.88 (s, 3H), 3.70 (s, 2H), 2.94 (m, 2H). Formula: C₁₁H₁₆NO₃Se, Calculated mass 289.2. MS (ESI⁺): *m/z* 290.2.

Synthesis of N-9-Fluorenylmethoxycarbonyl-Se-4-methoxybenzylselenocystein (Fmoc-SeCys(MBzl))



Scheme 2. Synthesis of N-9-Fluorenylmethoxycarbonyl-Se-4-methoxybenzylselenocystein (Fmoc-SeCys(MBzl)) from SeCys(MBzl)

To a suspension of SeCys(MBzl) (150 mg, 0.517 mmol) in water (2 mL) was added 1 eq. of triethylamine (TEA) at room temperature. Subsequently Fmoc-OSu, solubilized in CH₃CN (2 mL), was added dropwise to the reaction mixture.

Another equivalent of TEA and 6 mL supplementary of CH₃CN were added to obtain a clear solution (about 8 mL). The solution was left under stirring at room temperature for 1.5 h (monitored by silica TLC, DCM / CH₃OH 9: 1, R_f Product = 0.5).

It was acidified with 1N HCl (1.5 mL) and extracted with ethyl acetate (3x20 mL). The organic extracts were combined, washed with brine (high-concentration solution of NaCl), anhydriified with Na₂SO₄ and dried under vacuum. The obtained oily residue was purified by chromatography on Silica Gel 60, 0.075-0.2 mm (70-200 mesh) packed in column (40 cm x 5 cm). The elution was performed by 100% CHCl₃ to remove impurities and subsequently by a mixture of CHCl₃/CH₃OH

9.5: 0.5 v/v. The obtained pure white solid was characterized by ^1H and ^{13}C NMR in $(\text{CD}_3)_2\text{SO}$ (Figures S13 and S14, respectively).

^1H NMR (400 MHz, $(\text{CD}_3)_2\text{SO}$) δ 7.90 (d, $J = 7.5$ Hz, 2H), 7.74 (d, $J = 7.8$ Hz, 2H), 7.42 (t, $J = 7.4$ Hz, 2H), 7.32 (ddd, $J = 9.1, 5.2, 1.8$ Hz, 2H), 7.21 (d, $J = 8.5$ Hz, 2H), 6.84 (d, $J = 8.5$ Hz, 2H), 4.34-4.15 (m, 4H), 3.80 (s, 2H), 3.72 (s, 3H), 2.86-2.70 (m, 2H). ^{13}C NMR (101 MHz, $(\text{CD}_3)_2\text{SO}$) δ 172.86, 158.40, 156.40, 144.26, 141.18, 131.64, 130.36, 128.12, 127.55, 125.77, 120.59, 114.24, 66.19, 55.48, 55.01, 47.08, 26.76, 24.84.

^1H NMR and ^{13}C NMR spectra were acquired with Bruker 400 MHz.

Solid phase peptide synthesis of (S-Se)-AVP

The peptide was synthesized manually *via* Fmoc protocol on a 0.1 μmol scale using Rink amide resin (0.78 mmol/g) by incorporating into the sequence the synthesized Fmoc-SeCys(MBzl). All Fmoc-protected residues were added stepwise to the batch using fivefold excess of Fmoc aminoacid, HBTU and HOBT (by 5-min preactivation) in 0.2 M DIEA/DMF two times for 2 h. Fmoc deprotections were achieved using 20% piperidine/DMF for two times for 5 min under stirring at room temperature. The coupling and the Fmoc deprotection for each residue were monitored by ninhydrin reaction with primary amines developing an intense blue color (Kaiser test⁴²). Cleavage of peptide from the resins was carried out adapting the method reported by R. J. Hondal *et al.*⁴³: 8 h at room temperature under stirring with a cleavage cocktail (1 mL of mixture for g of resin) made by m-cresol/thioanisole/trifluoroacetic acid/trimethylsilyl trifluoromethanesulfonate (50:120:690:194). Then, the mixture was filtered from the resin and evaporated to one tenth of its original volume under a stream of nitrogen followed by precipitation of peptide into cold anhydrous diethyl ether. Crude peptide was lyophilized and then purified by

HPLC as outlined below. Pure peptide was lyophilized recovering 50 mg (42.4% Yield) and analyzed by ESI-MS (Figures S15 and S16). We found the expected value of $[M+H]^+ = 1132.3887$ Da ; $[M+2H]^{2+} = 566.6982$ Da.

Preparative HPLC was carried out on a LC8 Shimadzu HPLC system (Shimadzu Corporation, Kyoto, Japan) equipped with a UV lambda-Max Model 481 detector using a Phenomenex (Torrance, CA) C18 (300 Å, 250x21.20 mm, 5µ) column eluted with H₂O/0.1% TFA (A) and ACN/0.1% TFA (B) from 20-80% over 15 min at a flow rate of 20 mL·min⁻¹.

Purity of products was assessed using analytical HPLC (Agilent), column: C18-Phenomenex eluted with an H₂O/0.1 % TFA (A) and ACN/0.1 % TFA (B) from 5 % to 80 % over 20 minutes at 1 mL/min flow rate.

LC-MS STUDY

Sample preparation

Stock solutions of AVP, (Se-Se)-AVP, (S-Se)-AVP 0.9 mM and DTT 0.2 M were prepared by dissolving the samples in ultrapure water. Ammonium acetate buffer solution (2 mM, pH 7.0) was prepared by weighing ammonium acetate and dissolving it in ultrapure water, pH adjustment was carried out with acetic acid and ammonia commercial solutions (35% NH₃). For the incubation with mercury (II) compounds, 10 mM stock solutions of CH₃HgCl and HgCl₂ were prepared by dissolving salts in ultrapure water (0.1% HCl). For the pre-reduction of peptides, aliquots of their stock solution were diluted with 2 mM ammonium acetate solution (pH 7.0) to 0.1 mM final peptide concentration. Then, aliquots of DTT stock solution were added to achieve peptide to reducing agent ratios of 1:10 (final concentration of 1 mM of reducing agent) and the mixtures were

incubated for 30 minutes at 37 °C in a water bath under stirring. Thereafter, aliquots of CH₃HgCl and HgCl₂ stock solution were added to achieve peptide to Hg ratios of 1:1, 1:2 and 1:3 (0.1 mM, 0.2 mM and 0.3 mM, Hg concentration respectively). Those mixtures were explored over different incubation times (from 30 min up to 18 h) at 37 °C.

After the incubation, all mercury (II) incubated solutions were sampled and diluted to a final peptide concentration of 6 μM, using 2 mM ammonium acetate pH 7, 5 % (v/v) of ACN and 0.1 % (v/v) FA used for LC-MS analysis.

For the incubation with Hg₂Cl₂, a saturated stock solution was prepared by dissolving 0.1 mg of calomel in 50 mL of ultrapure water (4.2 μM Hg₂Cl₂ concentration). Then, 1 mL of this solution was mixed with 14 μL of reduced peptide at 0.1 mM in 2 mM ammonium acetate solution pH 7 (approximately, 1:3, peptide to Hg(I) ratio), incubated for 18 h and then analysed by LC-MS.

For the competitive study, the same starting solutions of peptides and CH₃HgCl were used and the same peptide concentration was employed for both incubation and LC-MS analysis.

LC-ESI MS

Separation and identification of our samples was performed by LC-ESI MS. Liquid chromatography separations were performed using Dionex ultimate 3000 series UHPLC (Thermo Fisher Scientific) coupled to an Orbitrap Q-Exactive Plus Mass Spectrometer (Thermo Fisher Scientific). The used column was AcclaimTM 120 (C18, 5 μm, 120 Å, 4.6 mm × 100 mm) (Thermo Fisher Scientific). The mobile phases were A, H₂O, and B, ACN, both with 0.1% FA. The flow rate used in all LC-MS experiments was 1 mL·min⁻¹, and sample elution was performed by using the gradient from 5% to 95% of B over 6.5 min. An injection volume of 10 μL was used.

Ionization was performed using an Electrospray ion source operating in positive ion mode with a capillary voltage of 3.80 kV and capillary temperature 400 °C. Sheath gas, auxiliary gas and sweep gas flow rate were set at 75, 20 and 1 (arbitrary units), respectively. Auxiliary gas temperature was set at 500 °C.

For each studied mass, a set of MS/MS spectra were acquired using an isolation width of 1.0 and 7.0 m/z, and a screening of collision energies (from 10 to 40 values of Higher-energy collisional dissociation (HCD)) was carried out. All MS data were analysed using from Thermo Fisher Scientific Xcalibur the Qual Browser and FreeStyle software.

LC-ICP MS

Using the same chromatographic delivery system as previously described in the LC-ESI MS methodology, the Dionex ultimate 3000 series UHPLC pump was coupled to a NexION 5000 ICP MS (Perkin Elmer) fitted with platinum cones. The exit of the column was connected to the nebulizer of the multiquadrupole ICP MS instrument, which allowed us to work in MS/MS mode. Employed carrier gas and option gas flow (O₂, used for avoiding carbon deposition from organic mobile phase) were 0.78 and 0.08 ml·min⁻¹, respectively. Hg was analyzed in “on-mass mode”, i.e. filtering the m/z=202 in Q1 and Q3, and RPq 0.25; while Se was analyzed in “mass-shift” mode, filtering the m/z=80 in Q1 and m/z=96 in Q3 after reaction with O₂, and RPq 0.8. The total acquisition time was 600 s.

Data Treatment

On the base of the comparison of the ICP and ESI detection modes for the CH₃HgCl induced metallation of (Se-Se)-AVP (Figure 4), correction factors were calculated and applied for

presenting relative abundance of XIC data, also for AVP and (S-Se)-AVP peptides, by extrapolation. Indeed, direct ICP-MS evaluation could not be performed directly for the reactivity study of these two peptides with mercury compounds, in the case of (S-Se)-AVP because of its limited quantity and, in the case of AVP, because the S based ICP quantification was hampered by the large presence of DTT in the reaction medium. The correction factors were calculated as follow: 0.76 for **1** (unreacted peptide), 5.25 for **2** (Hg-bridged peptide), 0.88 for **3** (bis-metallated adduct) and 2.30 for **4** (monometallated peptide). The latter value was calculated as the average of the three other values. These correction factors were applied to the relative abundances in Figures **20-22**, **S24-26** and **S32** in order to make the graphics of Figure **4-5**.

RESULTS AND DISCUSSION

The principle of the LC-MS/MS approach

As depicted in Figure **2**, the three model AVP peptides were pre-treated (30 min at 37°C) with the reducing agent dithiothreitol (DTT) and then reacted at physiological conditions (pH 7 and 37 °C) with HgCl₂, CH₃HgCl, or Hg₂Cl₂ (calomel), at different peptide/Hg molar ratios (from 1 to 3 equiv) and incubation times (from 30 min to 18 h) leading to several metal-peptide adducts (Table **1** and Table **S1**).

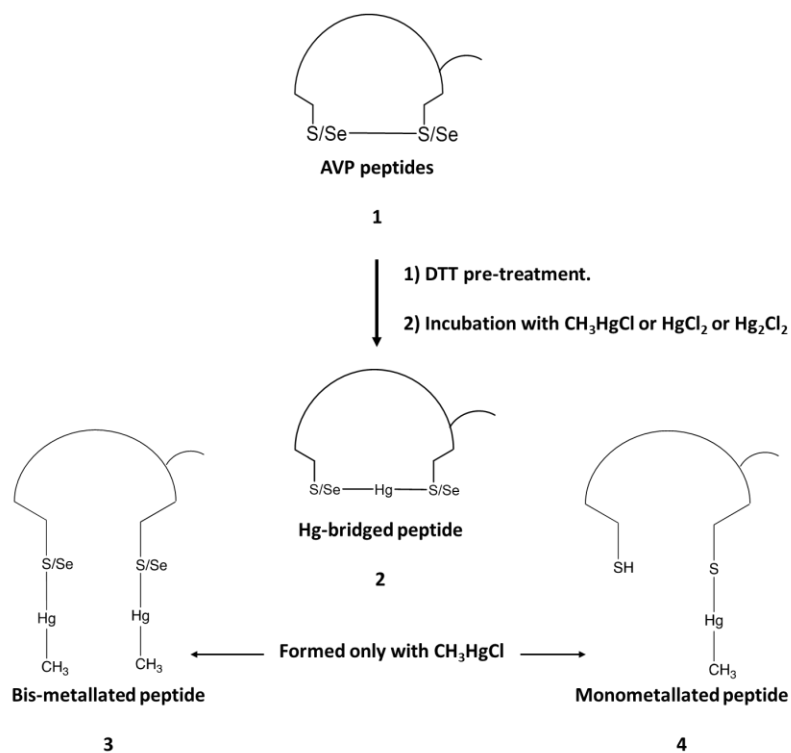


Figure 2. Scheme of the experiments: AVP peptides incubation with CH_3HgCl or HgCl_2 or Hg_2Cl_2 promoting, in the presence of DTT, the formation of Hg-bridged peptide adducts and, with CH_3HgCl , also the mono- and bis-metallated complexes.

Table1. AVP peptides and their Hg adducts identified by mass spectrometry after incubation of the peptides with HgCl₂ or CH₃HgCl or Hg₂Cl₂.

Peptide	Formula	Theoretical mass of the most	Experimental mass of the most	$\Delta M_{\text{theor-exp}}$ Da
		abundant isotope (Se ^{79.9160} and Hg ^{201.9701}) Da	abundant isotope (Se ^{79.9160} and Hg ^{201.9701}) Da	
AVP	C ₄₆ H ₆₅ N ₁₅ O ₁₂ S ₂	1083.4373	1083.4368	0.0005
Reduced AVP	C ₄₆ H ₆₇ N ₁₅ O ₁₂ S ₂	1085.4530	1085.4525	0.0005
Hg-bridged AVP ^a	C ₄₆ H ₆₅ HgN ₁₅ O ₁₂ S ₂	1285.4083	1285.4090	-0.0007
Bis-metallated AVP ^b	C ₄₈ H ₇₁ Hg ₂ N ₁₅ O ₁₂ S ₂	1515.4243	1515.4236	0.0007
Monometallated AVP ^b	C ₄₇ H ₆₉ HgN ₁₅ O ₁₂ S ₂	1301.4397	1301.4525	-0.0128
(Se-Se)-AVP	C ₄₆ H ₆₅ N ₁₅ O ₁₂ Se ₂	1179.3274	1179.3266	-0.0009
Hg-bridged (Se-Se)-AVP ^a	C ₄₆ H ₆₅ HgN ₁₅ O ₁₂ Se ₂	1379.2980	1379.2978	0.0002
Bis-metallated (Se-Se)-AVP ^b	C ₄₈ H ₇₁ Hg ₂ N ₁₅ O ₁₂ Se ₂	1609.3147	1609.3123	0.0024
(S-Se)-AVP	C ₄₆ H ₆₅ N ₁₅ O ₁₂ SSe	1131.3822	1131.3804	0.0018
Hg-bridged (S-Se)-AVP ^a	C ₄₆ H ₆₅ HgN ₁₅ O ₁₂ SSe	1331.3525	1331.3526	-0.0001
Bis-metallated (S-Se)-AVP ^b	C ₄₈ H ₇₁ Hg ₂ N ₁₅ O ₁₂ SSe	1563.3700	1563.3493	0.0207
Monometallated (S-Se)-AVP ^b	C ₄₇ H ₆₉ HgN ₁₅ O ₁₂ SSe	1347.3839	1347.3635	0.0204

^a Formed with HgCl₂, CH₃HgCl and Hg₂Cl₂.

^b Formed only with CH₃HgCl.

The reaction products were monitored and identified by LC-MS/MS (Figures **S17-19**, **S23-25** and **S29-31**), their identification was also complemented by comparison of experimental and theoretical isotopic patterns (Figure **S1-8**). The typical set of results (an example is shown in Figure **3** for (Se-Se)-AVP incubated with CH₃HgCl (1equiv, 30 min)), consisted of a total ion current chromatogram (TIC), mass spectra taken at the peak apexes (MS), the relative intensity of each species at their characteristic m/z values (extracted ion chromatogram, XIC) and their MS/MS spectra used to elucidate the metal binding sites. In brief, in Figure **3**, the TIC peaks 1, 2 and 3 (Figure **3A**) were identified in the mass spectra (Figure **3C-E**) as the unreacted, the Hg-bridged and the bis-metallated (Se-Se)-AVP peptide, respectively. The MS/MS of bis-metallated peptide (Figure **3F**) revealed the direct involvement of Se in the binding with mercury. Moreover, on the basis of the intensity of

the XIC of each species ($z=2$) (Figure 3B), we were able to assess the relative abundance of each of these peptides in the reaction medium as follows: $51 \pm 1.6\%$ of **3** (bis-metallated adduct), $45 \pm 1.7\%$ of **1** (unreacted peptide), $4.0 \pm 0.2\%$ of **2** (Hg-bridged peptide), these standard deviation values were found lower than expected.

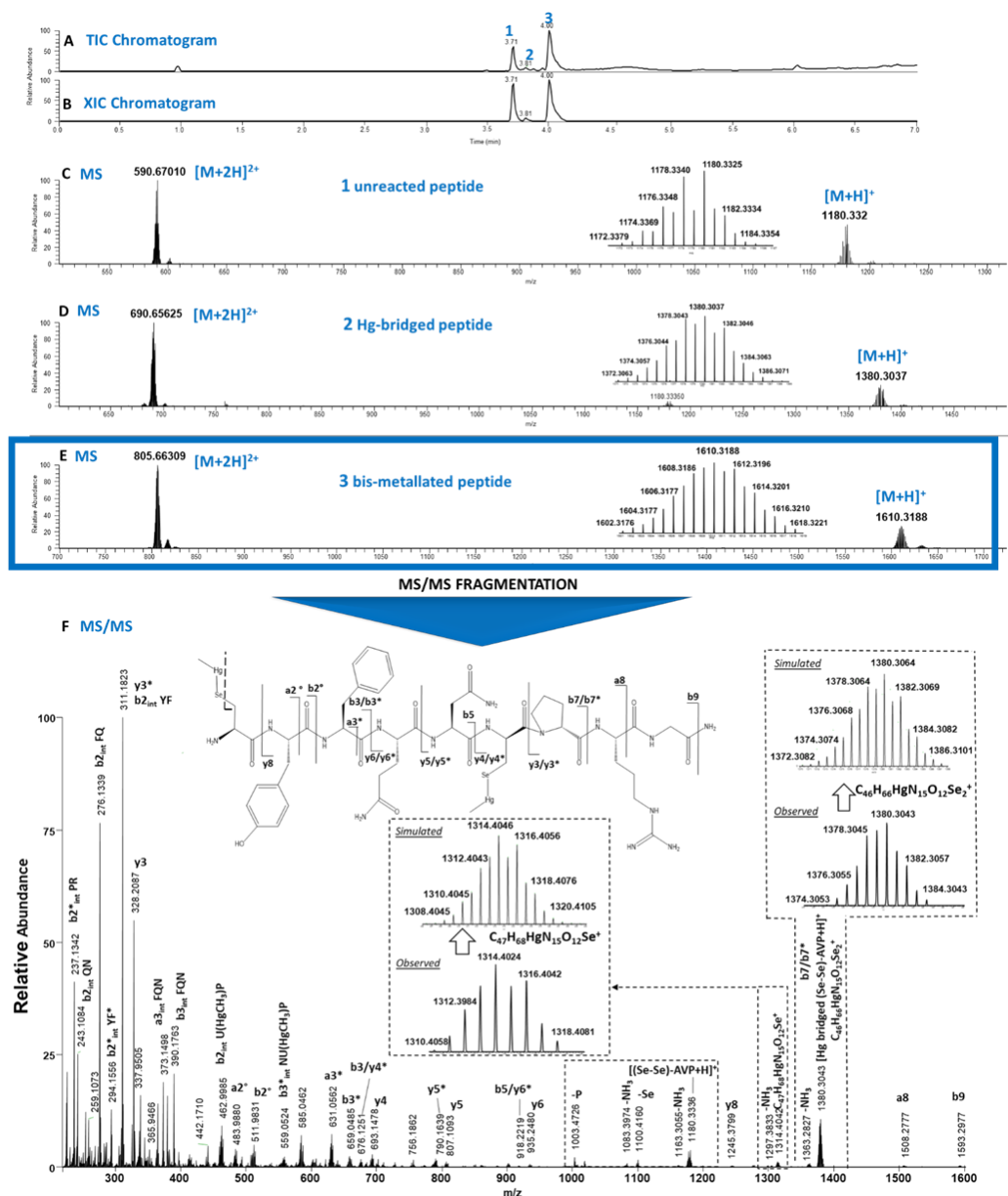


Figure 3. LC-MS of (Se-Se)-AVP incubated with 1 equiv of CH_3HgCl at 37°C in the presence of DTT during 30 min. (A) TIC. (B) XIC of ions m/z 590.67 ($z=2$, **1** unreacted peptide, $t_R=3.69$), 690.65 ($z=2$, **2** Hg-bridged peptide, $t_R=3.79$) and 805.66 ($z=2$, **3** bis-metallated peptide, $t_R=3.99$). (C-E) MS spectra of **1** unreacted peptide, $t_R=3.69$, **2** Hg-bridged

peptide, $t_R=3.79$ and **3** bis-metallated peptide, $t_R=3.99$, respectively. **(F)** MS/MS of **3** bis-metallated peptide at m/z 1610.3190 ($z=1$), principal fragments at HCD = 30.

This approach was integrated with inductively coupled plasma mass spectrometry (ICP-MS) detection in liquid chromatography (LC-ICP-MS) of the same reaction medium:⁴⁰ in Figure 4, the LC-ICP-MS Se and Hg profiles are superimposed to that obtained by LC-ESI-MS analysis (XIC). In contrast to ESI MS detection, ICP-MS is an element specific detector offering a response independent of the molecular structure. In fact, although the relative proportionality between the unreacted and metallated adducts is respected in the two detection modes, some differences are observed, especially for the Hg-bridged adduct. These differences were taken into account as described in the experimental section (Data Treatment) in order to give the relative abundances of each species in the graphics of Figures 4-6.

Note that metallation took place only when the peptides were pre-treated with DTT. This classical reduction protocol, which was tested to promote the reactivity of free selenols and thiols with mercury compounds, was able to reduce the disulfide bond of AVP, but not the diselenide bond⁴⁴ nor the S-Se bond. Our results therefore demonstrate the synergistic effect of DTT in promoting the reaction of Se with different Hg compounds when still present in the Se-Se form rather than in the selenol form. A competitive reactivity of DTT with the tested mercury compounds was found only in the case of AVP peptides incubations with CH_3HgCl : only traces of DTT-Hg adduct formation were detected in these reaction media (Figures S17-19 and S9-10).

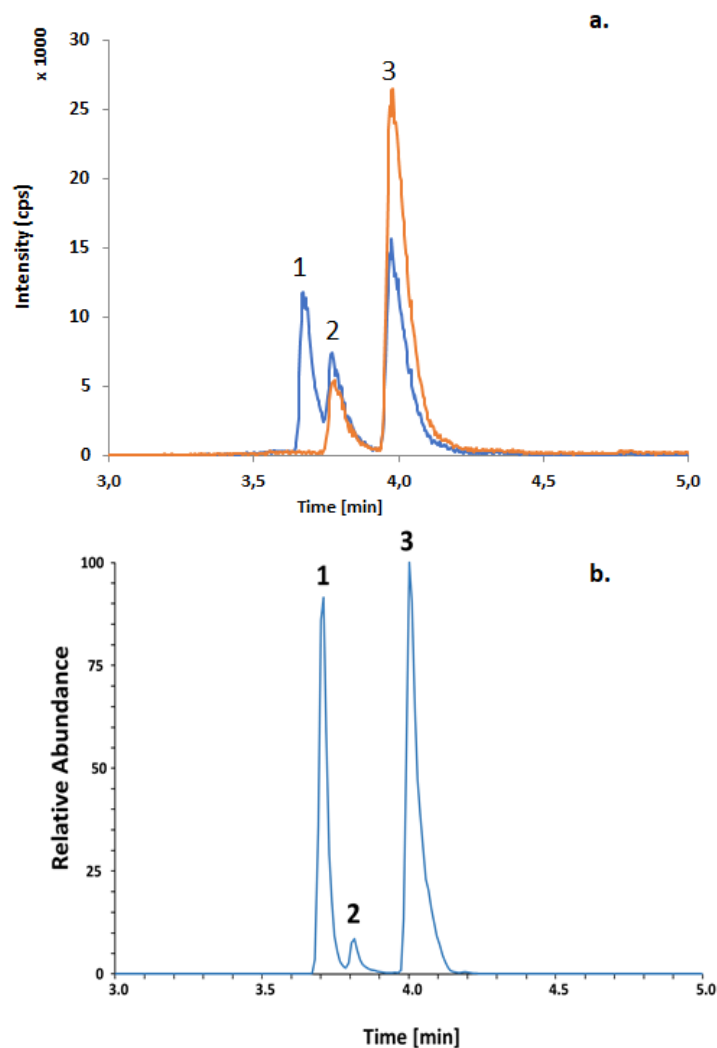


Figure 4. LC-ESI MS and LC-ICP MS/MS of (Se-Se)-AVP incubated with 1 equiv of CH₃HgCl at 37°C in presence of DTT during 30 min. **(a)** ICP-MS/MS detection: Se (blue line ⁹⁶Se ICP intensity) and Hg (orange line ²⁰²Hg ICP intensity). **(b)** ESI-MS detection: XIC of ions m/z 590.67 (**1** unreacted peptide, t_R= 3.71 min), 690.65 (**2** Hg-bridged peptide, t_R= 3.81 min) and 805.66 (**3** bis-metallated peptide, t_R= 4.00 min).

AVP peptides reactivity with CH₃HgCl

The reaction of the three AVP peptides with CH₃HgCl produced the mono-, bis-metallated and the Hg-bridged adducts (cf. Figure 2). These adducts were characterized by MS/MS revealing the direct involvement of Cys and SeCys in the binding with mercury (Figures S37-45).

Figure 5 shows for each peptide the relative abundance of unreacted and metallated peptides as a function of the number of CH₃HgCl equivalents at the different reaction times. These percentages were measured on the basis of the intensity of the extracted ion chromatogram for each reaction product (m/z with z=2) (Figures S20-22), by applying the ICP related corrections factors as previously described.

The results of AVP metallation were similar at the different incubation times, the peptide was mainly transformed into **4**: the monometallated peptide adduct. By increasing the excess of CH₃HgCl, the conversion of the starting peptide into the monometallated adduct increased (at 18 h, from 38 % to 70 %, with 1 equiv and 3 equiv, respectively), but unreacted peptide **1** still remained (17 %) after 18 h incubation with 3 equiv of CH₃HgCl.

(Se-Se)-AVP was largely converted into Hg adducts already at 30 min of incubation in the presence of 1 equiv of CH₃HgCl: In this reaction medium, 34 % of the peptide still remained unreacted while the bis-metallated adduct **3** was largely formed (44 %) together with the Hg-bridged form **2** (22 %). At any reaction time, when the excess of CH₃HgCl increased, the starting peptide reacted almost completely and the quantity of the bis-metallated adduct decreased by favouring the formation of the Hg-bridged peptide **2** (96, 100 and 99 % with 3 equiv of CH₃HgCl after 30 min, 3 h and 18 h of incubation, respectively).

The (S-Se)-AVP peptide showed an almost quantitative conversion into Hg adducts after 30 min of incubation with 1 equiv of CH₃HgCl by forming similar quantities of the Hg-bridged peptide **2**, the mono- **4** and bis-metallated **3** adducts (29, 31 and 33 %, respectively). Like in the case of (Se-Se)-AVP, at longer incubation time, the Hg-bridged peptide **2** represented the most predominant

form of Hg-peptide adduct (65, 80 and 86 % with 3 equiv of CH_3HgCl after 30 min, 3 h and 18 h of incubation, respectively).

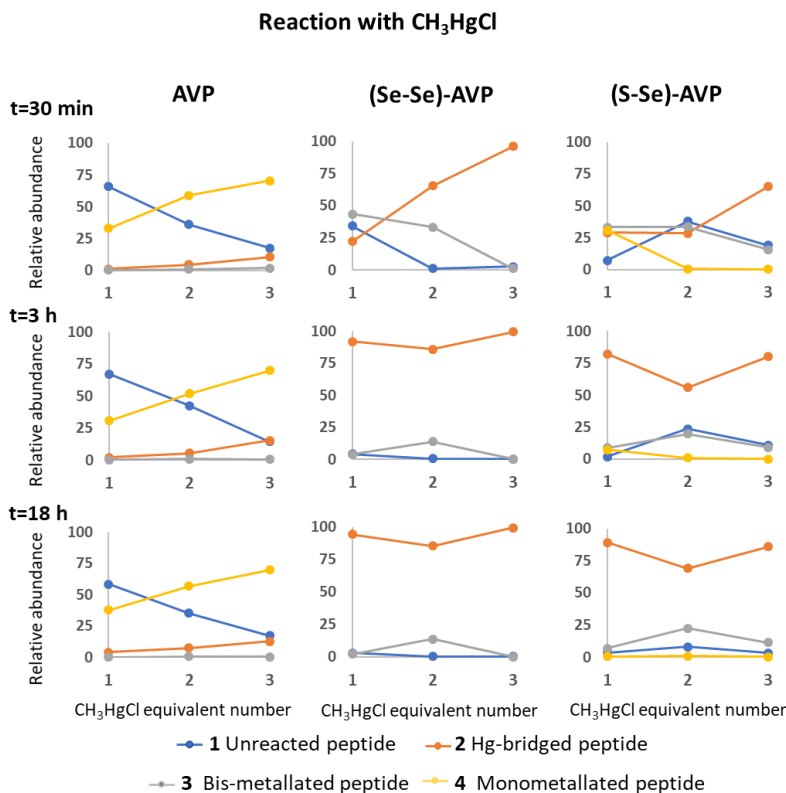


Figure 5. AVP peptides incubated at 37 °C in the presence of DTT with CH_3HgCl (1 to 3 equiv) at 30 min, 3 h and 18 h. Percentage of unreacted and metallated peptides are reported as a function of CH_3HgCl excess at the different reaction times.

AVP peptides reactivity with HgCl_2

The reaction of the three AVP peptides with HgCl_2 produced exclusively the Hg-bridged adduct **2** (cf. Figure 2).

Figure 6 shows for each peptide the relative abundance of unreacted peptide and Hg-bridged adduct as a function of the number of HgCl_2 equiv at the different reaction times. These percentages were measured on the basis of the intensity of the extracted ion chromatogram of each reaction product

(m/z with $z=2$) (Figures S26-28), by applying the ICP related corrections factors as previously described.

AVP showed similar reactivity profiles regardless of the excess of HgCl_2 or of the reaction time: the metallation was almost quantitative.

(Se-Se)-AVP was not totally metallated even in the presence of a threefold excess of HgCl_2 after 30 min or 3 h of incubation, (32 and 62 %, respectively). This peptide it needed longer incubation time to be almost more totally metallated: 98 % at 18 h of incubation with 3 equiv of HgCl_2 .

(S-Se)-AVP, as well as AVP, showed high conversion to the Hg-bridged adduct (above 78 %) at any excess of HgCl_2 or reaction time.

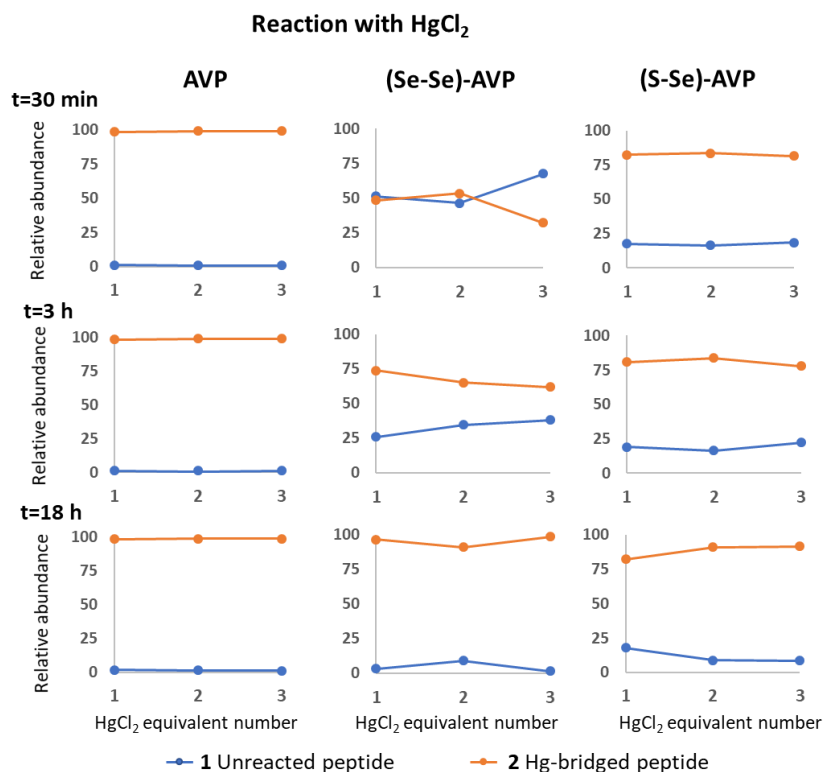


Figure 6. AVP peptides incubated at 37 °C in the presence of DTT with HgCl_2 (1 to 3 equiv) at 30 min, 3 h and 18 h: % of unreacted and Hg-bridged peptides are reported as function of HgCl_2 excess at the different reaction time.

AVP peptides reactivity with Hg₂Cl₂

In the case of Hg₂Cl₂, experiments were hampered by the low solubility of calomel in aqueous solution⁴⁵ making impossible the precise control of Hg excess at low concentrations. Therefore, incubations were performed exclusively in the presence of an excess of calomel (approximately, 3 equiv, at 4.2 μM concentration) during 18 h.

Under these conditions the AVP peptide remained almost unreacted while high amounts of (Se-Se)- and (S-Se)-AVP were largely converted into the Hg-bridged adducts (Figure S32 and Figure 7C). The formation of Hg-bridged peptide structures, after peptide incubation with calomel, indicated the change of Hg oxidation state from +1 to +2, as postulated by Heyrovsky for an excess of Cys addition after the formation of the Hg₂Cys₂ complex.²⁵ The presence of DTT in the reaction medium can also promote the disproportionation of Hg(I) to Hg(0) and Hg(II),^{46,47} followed by the subsequent complexation of Hg(II) to Se peptides.

Comparative reactivity of AVP peptides with mercury

Figure 7 compares the reactivity of AVP peptides incubated for 18 h with 3 equiv of different mercury compounds. For each peptide, the proportion between the unreacted form and the sum of metallated forms is shown.

~~CH₃HgCl was able to metallate 83, 100 and 97 % of AVP, (Se-Se) AVP and (S-Se) AVP, respectively. The main metallated forms were: monometallated AVP and the Hg-bridged adduct of (Se-Se) AVP and (S-Se) AVP.~~

Consequently, It was concluded that the replacement of S by Se in vasopressin significantly increased its reactivity towards CH_3HgCl while

HgCl_2 induced the formation of the Hg-bridged adduct of AVP, (Se-Se)-AVP and (S-Se)-AVP at 99, 98 and 91 %, respectively. HgCl_2 did not favour its reaction with the Se peptide over the S peptide, as it was observed for CH_3HgCl .

In the case of Hg_2Cl_2 , which almost did not react with AVP while converting high amount of (Se-Se)- and (S-Se)-AVP into the corresponding Hg-bridged species (95 and 93 %, respectively), the presence of at least one SeCys in the sequence of AVP seems to be essential for the metallation to occur.

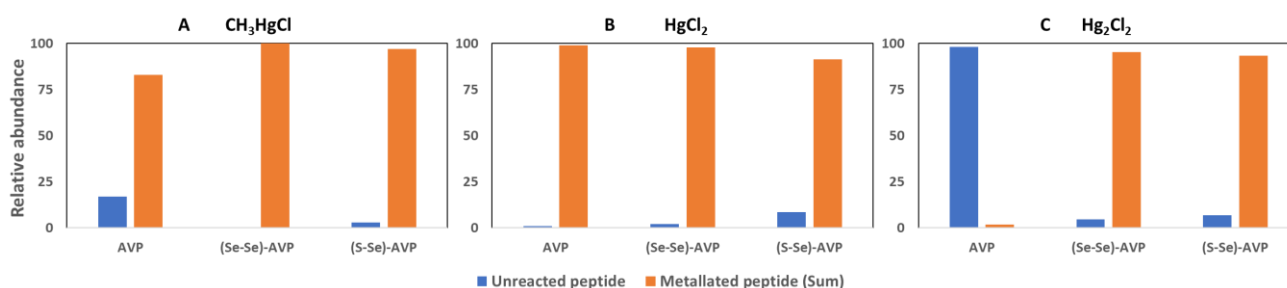


Figure 7. Relative abundance of unreacted and metallated (sum of adducts) AVP peptides incubated for 18 h at 37 °C in presence of DTT with 3 equiv of (A) CH_3HgCl (B) HgCl_2 or (C) Hg_2Cl_2 .

Proposed reaction mechanism

The comparison of the reactivity of AVP peptides towards HgCl_2 and CH_3HgCl showed that, while HgCl_2 produced only bridged adducts, CH_3HgCl also induced mono- and/or bis-metallation. The propensity of HgCl_2 to form exclusively bridged adducts is probably related to the good leaving group ability of the second chloride ligand, while the C-Hg bond in CH_3HgCl cannot be readily hydrolyzed. Indeed, CH_3HgCl induced also the mono- or bis-metallation, **4** and **3**, respectively

(Figure 8). Note that, in the case of (Se-Se)-AVP, the formation of the Hg-bridged adduct **2** was favored by an increase in the reaction time and an excess of CH_3HgCl .

After prolonged incubation time with CH_3HgCl , AVP formed almost exclusively the monometallated adduct **4**, while (S-Se)-AVP, as well as (Se-Se)-AVP, was converted into both the bis-metallated **3** and Hg-bridged **2** (prevalent) peptides. This underlies the high propensity of Se to promote a second reaction of the peptide with CH_3HgCl , by either an intramolecular- or intermolecular- reaction, like in the case of the Hg-bridged **2** and bis-metallated **3** adduct formation, respectively.

Notably, this comparative analysis of the reactivity of the vasopressin analogues with CH_3HgCl suggests that the replacement of S by Se promotes the conversion of vasopressin into the Hg-bridged adduct by demethylation of CH_3HgCl .⁴⁸

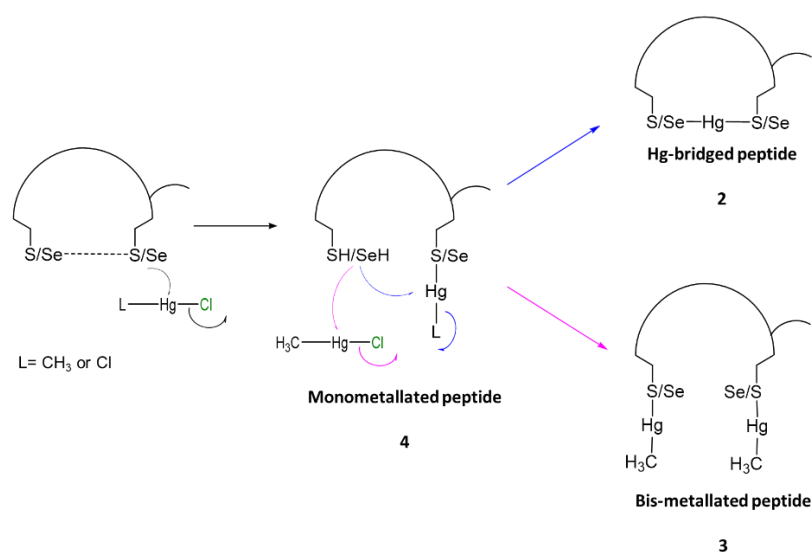


Figure 8. Proposed mechanism for the formation of Hg adducts with AVP peptides after reaction with CH_3HgCl and HgCl_2 compounds.

Competitive reactivity study

In order to assess the competition between S and Se forms of the peptide with CH_3HgCl , equimolar quantity of AVP (1 equiv), (Se-Se)-AVP (1 equiv) (both pre-treated with DTT) and CH_3HgCl (1 equiv) were simultaneously reacted at 37 °C for a time between 30 min and 18 h.

In the presence of its diselenide homologue, AVP was only slightly metallated, while the (Se-Se)-AVP was converted into the Hg-bridged **2** and the bis-metallated **3** adducts whose ratio increased over incubation time (Figure **S33**).

The same experiment was repeated in the presence of higher quantities of AVP: 10-fold and 50-fold molar excess with respect to (Se-Se)-AVP (1 equiv) and CH_3HgCl (1 equiv). In the presence of 10-fold molar excess of AVP, diselenide vasopressin showed a high extent of metallation (Figure **S34**). Surprisingly, even in presence of a 50-fold molar excess of AVP, the (Se-Se)-AVP still competed with its disulfide homologue in the binding with CH_3HgCl (Figure **S35**).

In conclusion, at the equimolar ratio, (Se-Se)-AVP was found to be more reactive towards CH_3Hg^+ than AVP and, in the presence of much larger amount of the latter, it was still able to be metallated by CH_3HgCl . This observation prompted us to investigate the ability of (Se-Se)-AVP to displace the CH_3Hg -moiety from AVP. For this purpose, AVP (pre-reduced with DTT) was first incubated for 18 h with 1 equiv of CH_3HgCl in order to obtain its metallated adducts (Figure **9A**), and then treated for 30 min with 1 equiv of (Se-Se)-AVP (pre-treated with DTT) (Figures **S36** and **9B**). After 30 min of reaction, AVP almost totally lost the CH_3Hg -moiety bound to S (Figure **9B1**), while (Se-Se)-AVP formed the bis metallated and the Hg-bridged adducts (Figure **9B2**).

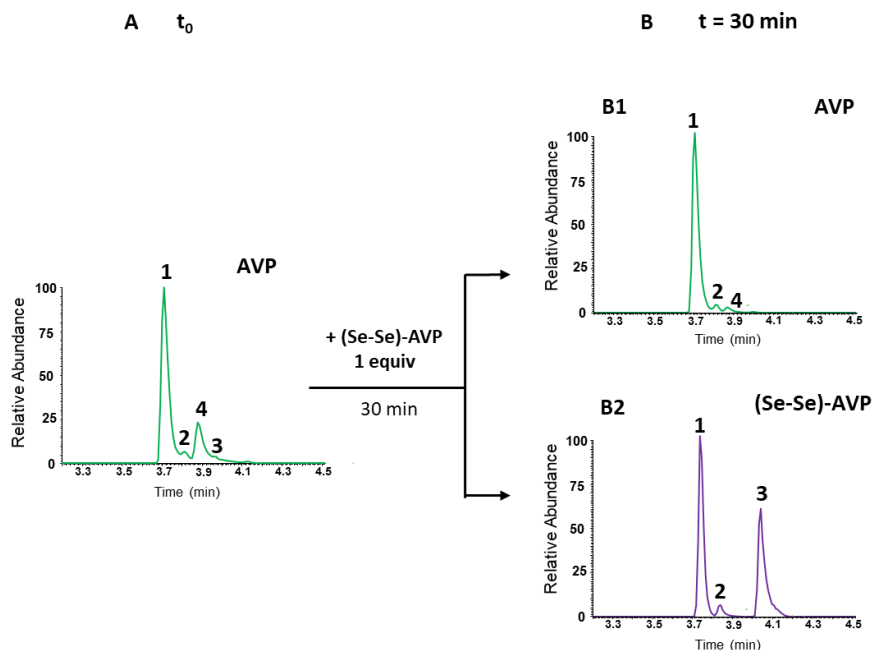


Figure 9. (A) LC-MS of AVP pre-treated with DTT and incubated with 1 equiv of CH₃HgCl at 37 °C during 18 h. XIC of ions m/z 542.72 (**1** AVP, t_R=3.69 min), 643.71 (**2** Hg-bridged AVP, t_R=3.78 min), 651,72 (**4** monometallated AVP adduct, t_R=3.87 min) and 758.72 (**3** bis-metallated AVP adduct, t_R=3.95 min). (B) LC-MS of pre-metallated AVP after incubation with 1 equiv of (Se-Se)-AVP at 37 °C during 30 min. (B1) XIC of AVP ions m/z 542.72 (**1** AVP, t_R=3.69 min), 643.71 (**2** Hg-bridged AVP, t_R=3.78 min) and 651,72 (**4** monometallated AVP adduct, t_R=3,87 min). (B2) XIC of (Se-Se)-AVP ions m/z 590,67 (**1** (Se-Se)-AVP, t_R=3.71 min), 690.65 (**2** Hg-bridged (Se-Se)-AVP, t_R=3.81 min) and 805.66 (**3** bis-metallated (Se-Se)-AVP, t_R=4.05).

CONCLUSION

In this first experimental study of the comparative reactivity of Cys- and SeCys-containing biomolecules with different Hg compounds, we show that the replacement of S by Se in vasopressin drastically increased its reactivity towards CH₃HgCl. The reaction of (Se-Se)-AVP favoured the formation of the Hg-bridged peptide by demethylation of CH₃HgCl. In competitive experiments, (Se-Se)-AVP readily and preferentially reacted with CH₃HgCl, showing a significant metallation extent even in the presence of a larger excess of its Cys homologue. Based on this result, we can hypothesize that this selenopeptide can interfere in the binding of CH₃Hg⁺ with protein thiols

primary target of Hg toxicity. Moreover, (Se-Se)-AVP was able to almost totally displace the CH₃Hg-moiety linked to S in AVP which opens a perspective of using diselenide peptides as CH₃Hg⁺ chelation agents. In fact, as analogue of the natural hormone with full activity retained towards the vasopressin receptor³⁷, (Se-Se)-AVP can represent a potential lead compound for the development of methylmercury detoxification strategies.

ASSOCIATED CONTENT

Supporting Information.

Table S1. List of observed MS products and their structure

Comparison of theoretical and experimental isotopic patterns.

Characterization of synthetic products (NMR and MS).

LC-MS of AVP peptides reactivity with mercury compounds.

MS/MS of Hg-peptide adducts.

The following files are available free of charge:

Supplementary Information(PDF)

AUTHOR INFORMATION

Corresponding Author

*Luisa Ronga

EMAIL: luisa.ronga@univ-pau.fr

Author Contributions

The manuscript was written through contributions of all authors. All authors have given approval to the final version of the manuscript.

ACKNOWLEDGMENT

M.B.M. acknowledges E2S-UPPA for the PhD fellowship. Financial support of the CNR for “The Bioinorganic Drugs (BIDs) joint laboratory: A multidisciplinary platform promoting new molecular targets for drug discovery” is acknowledged. Authors thank Dr. Simon Godin and Dr. Javier Jimenez Lamana for training M.B.M in ESI- and ICP-MS, respectively.

REFERENCES

- (1) Lamborg, C. H.; Hammerschmidt, C. R.; Bowman, K. L.; Swarr, G. J.; Munson, K. M.; Ohnemus, D. C.; Lam, P. J.; Heimbürger, L.-E.; Rijkenberg, M. J. A.; Saito, M. A. A Global Ocean Inventory of Anthropogenic Mercury Based on Water Column Measurements. *Nature* **2014**, *512* (7512), 65–68. <https://doi.org/10.1038/nature13563>.
- (2) Selin, N. E. Global Biogeochemical Cycling of Mercury: A Review. *Annu. Rev. Environ. Resour.* **2009**, *34* (1), 43–63. <https://doi.org/10.1146/annurev.envIRON.051308.084314>.
- (3) Petrova, M. V.; Ourgaud, M.; Boavida, J. R. H.; Dufour, A.; Tesán Onrubia, J. A.; Lozingot, A.; Heimbürger-Boavida, L.-E. Human Mercury Exposure Levels and Fish Consumption at the French Riviera. *Chemosphere* **2020**, *258*, 127232. <https://doi.org/10.1016/j.chemosphere.2020.127232>.
- (4) Xu, X.; Han, J.; Pang, J.; Wang, X.; Lin, Y.; Wang, Y.; Qiu, G. Methylmercury and Inorganic Mercury in Chinese Commercial Rice: Implications for Overestimated Human Exposure

and Health Risk. *Environmental Pollution* **2020**, 258, 113706.

<https://doi.org/10.1016/j.envpol.2019.113706>.

(5) Pearson, R. G. Hard and Soft Acids and Bases. *J. Am. Chem. Soc.* **1963**, 85 (22), 3533–3539. <https://doi.org/10.1021/ja00905a001>.

(6) Ajsuvakova, O. P.; Tinkov, A. A.; Aschner, M.; Rocha, J. B. T.; Michalke, B.; Skalnaya, M. G.; Skalny, A. V.; Butnariu, M.; Dadar, M.; Sarac, I.; Aaseth, J.; Bjørklund, G. Sulfhydryl Groups as Targets of Mercury Toxicity. *Coordination Chemistry Reviews* **2020**, 417, 213343. <https://doi.org/10.1016/j.ccr.2020.213343>.

(7) Quig, D. Cysteine Metabolism and Metal Toxicity. *Altern Med Rev* **1998**, 3 (4), 262–270.

(8) Starý, J.; Kratzer, K. Radiometric Determination of Stability Constants of Mercury Species Complexes with L-Cysteine. *Journal of Radioanalytical and Nuclear Chemistry Letters* **1988**, 126 (1), 69–75. <https://doi.org/10.1007/BF02164804>.

(9) Wang, F.; Lemes, M.; Khan, M. A. K. Metallomics of Mercury: Role of Thiol- and Selenol-Containing Biomolecules. In *Environmental Chemistry and Toxicology of Mercury*; Liu, G., Cai, Y., O'Driscoll, N., Eds.; John Wiley & Sons, Inc.: Hoboken, NJ, USA, 2011; pp 517–544. <https://doi.org/10.1002/9781118146644.ch16>.

(10) Sénèque, O.; Rousselot-Pailley, P.; Pujol, A.; Boturnyn, D.; Crouzy, S.; Proux, O.; Manceau, A.; Lebrun, C.; Delangle, P. Mercury Trithiolate Binding (HgS₃) to a de Novo Designed Cyclic Decapeptide with Three Preoriented Cysteine Side Chains. *Inorg. Chem.* **2018**, 57 (5), 2705–2713. <https://doi.org/10.1021/acs.inorgchem.7b03103>.

- (11) Mesterházy, E.; Lebrun, C.; Crouzy, S.; Jancsó, A.; Delangle, P. Short Oligopeptides with Three Cysteine Residues as Models of Sulphur-Rich Cu(I)- and Hg(II)-Binding Sites in Proteins. *Metallomics* **2018**, *10* (9), 1232–1244. <https://doi.org/10.1039/C8MT00113H>.
- (12) Ngu-Schwemlein, M.; Lin, X.; Rudd, B.; Bronson, M. Synthesis and ESI Mass Spectrometric Analysis of the Association of Mercury(II) with Multi-Cysteinyll Peptides. *Journal of Inorganic Biochemistry* **2014**, *133*, 8–23. <https://doi.org/10.1016/j.jinorgbio.2013.12.008>.
- (13) Steele, R. A.; Opella, S. J. Structures of the Reduced and Mercury-Bound Forms of MerP, the Periplasmic Protein from the Bacterial Mercury Detoxification System. *Biochemistry* **1997**, *36* (23), 6885–6895. <https://doi.org/10.1021/bi9631632>.
- (14) Rossy, E.; Sénèque, O.; Lascoux, D.; Lemaire, D.; Crouzy, S.; Delangle, P.; Covès, J. Is the Cytoplasmic Loop of MerT, the Mercuric Ion Transport Protein, Involved in Mercury Transfer to the Mercuric Reductase? *FEBS Letters* **2004**, *575* (1–3), 86–90. <https://doi.org/10.1016/j.febslet.2004.08.041>.
- (15) Ledwidge, R.; Patel, B.; Dong, A.; Fiedler, D.; Falkowski, M.; Zelikova, J.; Summers, A. O.; Pai, E. F.; Miller, S. M. NmerA, the Metal Binding Domain of Mercuric Ion Reductase, Removes Hg²⁺ from Proteins, Delivers It to the Catalytic Core, and Protects Cells under Glutathione-Depleted Conditions. *Biochemistry* **2005**, *44* (34), 11402–11416. <https://doi.org/10.1021/bi050519d>.
- (16) Faller, P.; Ctortocka, B.; Tröger, W.; Butz, T.; Vašák, M. Optical and TDPAC Spectroscopy of Hg(II)-Rubredoxin: Model for a Mononuclear Tetrahedral [Hg(CysS)₄]²⁻ Center. *J Biol Inorg Chem* **2000**, *5* (3), 393–401. <https://doi.org/10.1007/PL00010668>.

- (17) Chang, C.-C.; Lin, L.-Y.; Zou, X.-W.; Huang, C.-C.; Chan, N.-L. Structural Basis of the Mercury(II)-Mediated Conformational Switching of the Dual-Function Transcriptional Regulator MerR. *Nucleic Acids Res* **2015**, *43* (15), 7612–7623. <https://doi.org/10.1093/nar/gkv681>.
- (18) Song, S.; Li, Y.; Liu, Q. S.; Wang, H.; Li, P.; Shi, J.; Hu, L.; Zhang, H.; Liu, Y.; Li, K.; Zhao, X.; Cai, Z. Interaction of Mercury Ion (Hg²⁺) with Blood and Cytotoxicity Attenuation by Serum Albumin Binding. *Journal of Hazardous Materials* **2021**, *412*, 125158. <https://doi.org/10.1016/j.jhazmat.2021.125158>.
- (19) Simmons-Willis, T. A.; Koh, A. S.; Clarkson, T. W.; Ballatori, N. Transport of a Neurotoxicant by Molecular Mimicry: The Methylmercury–l-Cysteine Complex Is a Substrate for Human L-Type Large Neutral Amino Acid Transporter (LAT) 1 and LAT2. *Biochemical Journal* **2002**, *367* (1), 239–246. <https://doi.org/10.1042/bj20020841>.
- (20) Aschner, M.; Aschner, J. L.; Kimelberg, H. K. Methylmercury Neurotoxicity and Its Uptake Across the Blood — Brain Barrier. In *The Vulnerable Brain and Environmental Risks: Volume 2 Toxins in Food*; Isaacson, R. L., Jensen, K. F., Eds.; Springer US: Boston, MA, 1992; pp 3–17. https://doi.org/10.1007/978-1-4615-3330-6_1.
- (21) Kajiwara, Y.; Yasutake, A.; Adachi, T.; Hirayama, K. Methylmercury Transport across the Placenta via Neutral Amino Acid Carrier. *Archives of Toxicology* **1996**, *70* (5), 310–314. <https://doi.org/10.1007/s002040050279>.
- (22) Pochini, L.; Peta, V.; Indiveri, C. Inhibition of the OCTN2 Carnitine Transporter by HgCl₂ and Methylmercury in the Proteoliposome Experimental Model: Insights in the Mechanism of Toxicity. *Toxicology Mechanisms and Methods* **2013**, *23* (2), 68–76. <https://doi.org/10.3109/15376516.2012.719166>.

- (23) Galluccio, M.; Pochini, L.; Peta, V.; Ianni, M.; Scalise, M.; Indiveri, C. Functional and Molecular Effects of Mercury Compounds on the Human OCTN1 Cation Transporter: C50 and C136 Are the Targets for Potent Inhibition. *Toxicological Sciences* **2015**, *144* (1), 105–113. <https://doi.org/10.1093/toxsci/kfu259>.
- (24) Kanda, H.; Toyama, T.; Shinohara-Kanda, A.; Iwamatsu, A.; Shinkai, Y.; Kaji, T.; Kikushima, M.; Kumagai, Y. S-Mercuration of Rat Sorbitol Dehydrogenase by Methylmercury Causes Its Aggregation and the Release of the Zinc Ion from the Active Site. *Arch Toxicol* **2012**, *86* (11), 1693–1702. <https://doi.org/10.1007/s00204-012-0893-4>.
- (25) Heyrovský, M.; Mader, P.; Vavříčka, S.; Veselá, V.; Fedurco, M. The Anodic Reactions at Mercury Electrodes Due to Cysteine. *Journal of Electroanalytical Chemistry* **1997**, *430* (1–2), 103–117. [https://doi.org/10.1016/S0022-0728\(97\)00103-4](https://doi.org/10.1016/S0022-0728(97)00103-4).
- (26) Gajdosechova, Z.; Mester, Z.; Feldmann, J.; Krupp, E. M. The Role of Selenium in Mercury Toxicity – Current Analytical Techniques and Future Trends in Analysis of Selenium and Mercury Interactions in Biological Matrices. *TrAC Trends in Analytical Chemistry* **2018**, *104*, 95–109. <https://doi.org/10.1016/j.trac.2017.12.005>.
- (27) Ralston, N. V. C.; Raymond, L. J. Mercury's Neurotoxicity Is Characterized by Its Disruption of Selenium Biochemistry. *Biochimica et Biophysica Acta (BBA) - General Subjects* **2018**, *1862* (11), 2405–2416. <https://doi.org/10.1016/j.bbagen.2018.05.009>.
- (28) Carty, A.; Malone, S. F.; Taylor, N. J.; Canty', A. J. Synthesis, Spectroscopic, and X-Ray Structural Characterization of Methylmercury-D, L-Selenocysteinate Monohydrate, a Key Model for the Methylmercury(II)-Selenoprotein Interaction. *Journal of Inorganic Biochemistry* **1983**, *18* (4), 291–300. [https://doi.org/10.1016/0162-0134\(83\)85044-2](https://doi.org/10.1016/0162-0134(83)85044-2).

- (29) Taylor, N. J.; Wong, Y. S.; Chieh, P. C.; Carty, A. J. Syntheses, X-Ray Crystal Structure, and Vibrational Spectra of L-Cysteinato(Methyl)Mercury(II) Monohydrate. *J. Chem. Soc., Dalton Trans.* **1975**, No. 5, 438. <https://doi.org/10.1039/dt9750000438>.
- (30) Khan, M. A. K.; Asaduzzaman, A. Md.; Schreckenbach, G.; Wang, F. Synthesis, Characterization and Structures of Methylmercury Complexes with Selenoamino Acids. *Dalton Trans.* **2009**, No. 29, 5766. <https://doi.org/10.1039/b903863a>.
- (31) Asaduzzaman, A. Md.; Khan, M. A. K.; Schreckenbach, G.; Wang, F. Computational Studies of Structural, Electronic, Spectroscopic, and Thermodynamic Properties of Methylmercury-Amino Acid Complexes and Their Se Analogues. *Inorg. Chem.* **2010**, *49* (3), 870–878. <https://doi.org/10.1021/ic900827m>.
- (32) Valea, A.; Georgescu, C. E. Selenoproteins in Human Body: Focus on Thyroid Pathophysiology. *Hormones* **2018**, *17* (2), 183–196. <https://doi.org/10.1007/s42000-018-0033-5>.
- (33) Bernabeu de Maria, M.; Lamarche, J.; Ronga, L.; Messori, L.; Szpunar, J.; Lobinski, R. Selenol (-SeH) as a Target for Mercury and Gold in Biological Systems: Contributions of Mass Spectrometry and Atomic Spectroscopy. *Coordination Chemistry Reviews* **2023**, *474*, 214836. <https://doi.org/10.1016/j.ccr.2022.214836>.
- (34) Manceau, A.; Azemard, S.; Hédouin, L.; Vassileva, E.; Lecchini, D.; Fauvelot, C.; Swarzenski, P. W.; Glatzel, P.; Bustamante, P.; Metian, M. Chemical Forms of Mercury in Blue Marlin Billfish: Implications for Human Exposure. *Environ. Sci. Technol. Lett.* **2021**, *8* (5), 405–411. <https://doi.org/10.1021/acs.estlett.1c00217>.

- (35) Pickering, I. J.; Cheng, Q.; Rengifo, E. M.; Nehzati, S.; Dolgova, N. V.; Kroll, T.; Sokaras, D.; George, G. N.; Arnér, E. S. J. Direct Observation of Methylmercury and Auranofin Binding to Selenocysteine in Thioredoxin Reductase. *Inorg. Chem.* **2020**, *59* (5), 2711–2718. <https://doi.org/10.1021/acs.inorgchem.9b03072>.
- (36) Sugiura, Y.; Tamai, Y.; Tanaka, H. Selenium Protection against Mercury Toxicity: High Binding Affinity of Methylmercury by Selenium-Containing Ligands in Comparison with Sulfur-Containing Ligands. *Bioinorganic Chemistry* **1978**, *9* (2), 167–180. [https://doi.org/10.1016/S0006-3061\(00\)80288-4](https://doi.org/10.1016/S0006-3061(00)80288-4).
- (37) Cordeau, E.; Arnaudguilhem, C.; Bouyssiere, B.; Hagège, A.; Martinez, J.; Subra, G.; Cantel, S.; Enjalbal, C. Investigation of Elemental Mass Spectrometry in Pharmacology for Peptide Quantitation at Femtomolar Levels. *PLoS ONE* **2016**, *11* (6), e0157943. <https://doi.org/10.1371/journal.pone.0157943>.
- (38) Mobli, M.; Morgenstern, D.; King, G. F.; Alewood, P. F.; Muttenthaler, M. Site-Specific PKa Determination of Selenocysteine Residues in Selenovasoressin by Using ⁷⁷Se NMR Spectroscopy. *Angew. Chem. Int. Ed.* **2011**, *50* (50), 11952–11955. <https://doi.org/10.1002/anie.201104169>.
- (39) Wenzel, M.; Casini, A. Mass Spectrometry as a Powerful Tool to Study Therapeutic Metallodrugs Speciation Mechanisms: Current Frontiers and Perspectives. *Coordination Chemistry Reviews* **2017**, *352*, 432–460. <https://doi.org/10.1016/j.ccr.2017.02.012>.
- (40) Łobiński, R.; Schaumlöffel, D.; Szpunar, J. Mass Spectrometry in Bioinorganic Analytical Chemistry. *Mass Spectrom. Rev.* **2006**, *25* (2), 255–289. <https://doi.org/10.1002/mas.20069>.

- (41) Koide, T.; Itoh, H.; Otaka, A.; Yasui, H.; Kuroda, M.; Esaki, N.; Soda, K.; Fujii, N. Synthetic Study on Selenocystine-Containing Peptides. *Chemical & Pharmaceutical Bulletin* **1993**, *41* (3), 502–506. <https://doi.org/10.1248/cpb.41.502>.
- (42) Kaiser, E.; Colescott, R. L.; Bossinger, C. D.; Cook, P. I. Color Test for Detection of Free Terminal Amino Groups in the Solid-Phase Synthesis of Peptides. *Analytical Biochemistry* **1970**, *34* (2), 595–598. [https://doi.org/10.1016/0003-2697\(70\)90146-6](https://doi.org/10.1016/0003-2697(70)90146-6).
- (43) Hondal, R. J.; Nilsson, B. L.; Raines, R. T. Selenocysteine in Native Chemical Ligation and Expressed Protein Ligation. *J. Am. Chem. Soc.* **2001**, *123* (21), 5140–5141. <https://doi.org/10.1021/ja005885t>.
- (44) Lamarche, J.; Alcoceba Álvarez, E.; Cordeau, E.; Enjalbal, C.; Massai, L.; Messori, L.; Lobinski, R.; Ronga, L. Comparative Reactivity of Medicinal Gold(i) Compounds with the Cyclic Peptide Vasopressin and Its Diselenide Analogue. *Dalton Trans.* **2021**, *50* (47), 17487–17490. <https://doi.org/10.1039/D1DT03470G>.
- (45) Nikolaychuk, P. A. Is Calomel Truly a Poison and What Happens When It Enters the Human Stomach? A Study from the Thermodynamic Viewpoint. *Main Group Metal Chemistry* **2016**, *39* (1–2). <https://doi.org/10.1515/mgmc-2015-0040>.
- (46) Loux, N. T. An Assessment of Mercury-Species-Dependent Binding with Natural Organic Carbon. *Chemical Speciation & Bioavailability* **1998**, *10* (4), 127–136. <https://doi.org/10.3184/095422998782775754>.
- (47) Vitello, J. D.; Pistone, D.; Cormier, A. D. A Problem Associated with the Use of a Calomel Reference Electrode in an ISE Analytical System. *Scandinavian Journal of Clinical and*

Laboratory Investigation **1996**, *56* (sup224), 165–171.

<https://doi.org/10.3109/00365519609088636>.

(48) Khan, M. A. K.; Wang, F. Chemical Demethylation of Methylmercury by Selenoamino Acids. *Chem. Res. Toxicol.* **2010**, *23* (7), 1202–1206. <https://doi.org/10.1021/tx100080s>.

SYNOPSIS

The diselenium analog of the vasopressin hormone reacts with methylmercury (CH_3Hg^+) by forming a Hg-bridged peptide adduct by demethylation of CH_3Hg^+ . In competition experiments, CH_3Hg^+ reacts preferentially with the diselenium analogue rather than with vasopressin. The diselenium vasopressin also shows the capability to displace CH_3Hg^+ bound to S in vasopressin, opening a promising perspective for the use of selenopeptides for methylmercury chelation.

